18th International Conference on Information Fusion
Washington, DC - July 6-9, 2015

Joint tracking and classification based on kinematic and target extent measurements

Clement Magnant*†, Audrey Giremus†, Eric Grivel†, Laurent Ratton‡, Bernard Joseph*
Thales Airborne Systems S.A., * Pessac, ‡ Elancourt, FRANCE.
† University of Bordeaux – Bordeaux INP – IMS – UMR CNRS 5218, Talence, FRANCE

***Abstract*—A great deal of interest has been paid to target tracking for the last decades. When using Bayesian estimation algorithms, choosing relevant motion models is crucial for accurate localization. Information on the type of target and its maneuver capability can be helpful in the motion model design. Thus, joint tracking and classification (JTC) methods based on target features have been recently developed. In this paper, JTC is addressed by using target extent measurements. We present a flexible formulation of the JTC problem where a target class is characterized by a set of possible motion models. Two multiclass multiple-model algorithms are first derived. Then, to alleviate the difficult tuning of the model parameters, we take advantage of Bayesian non-parametric models. A Dirichlet-process based algorithm is presented for the JTC and the model parameter estimation. Finally, a comparative study of these three approaches is carried out for maritime-target tracking.**

***Keywords*—Joint tracking and classification (JTC), target extent, Bayesian estimation, multiple models, dirichlet process.**

I. Introduction

Among the functions performed by a surveillance radar, tracking algorithms allow targets to be located at each instant so that their evolutions can be observed by the user over time. In general, tracking is based on recursive Bayesian approaches such as Kalman filtering or particle filtering. In this case, the *a priori* choice of the motion model impacts the tracking accuracy. Taking into account information about the target type can help defining relevant models [1]–[5]. This is one of the reasons why joint tracking and classification (JTC) methods have been recently proposed.

Classically, the target classification is based on target features such as the shape, the size or the dynamical capabilities. In [6], Ristic *et al.* propose to use kinematic information to classify air targets. More particularly, all the target classes share the same dynamical model but differ by the span of possible accelerations. In [7], Challa *et al.* address the target classification issue by using both radar measurements and electronic support measures (ESM) data. Then, they present the corresponding Bayesian radar and ESM data fusion algorithm.

To our knowledge, the target size has not been considered yet as a target feature for JTC algorithms. In classical target tracking approaches, single-point measurements of the target position are used [7]–[9]. However, the target extent measurements, which are one-dimensional measurements of the target length along the radar-to-target line of sight (LOS) [10] [11], can be provided by recent sensors such as high-range resolution (HRR) radars. In [10], the authors suggest using this attribute in target tracking to improve the performance of classical data association algorithms. For this purpose, an elliptical target model is introduced so that target extent measurements can be exploited for any target orientation regarding the sensor-to-target direction. However, there is no classification in this method.

In this paper, JTC algorithms based on both kinematic measurements and target extent measurements are presented. A target is assumed to belong to one among several predefined target classes. Each class corresponds to a specific type of targets (small or large, cooperative or not, maneuvering or not, etc.). Conditionally to this class, contrary to [11], we suggest modeling the target dynamic by different motion models. The target class and the kinematic parameters are jointly estimated from both the noisy kinematic measurements and the target extent measurements. First, two multiclass multiple-model (MM) based Bayesian algorithms are derived. One is an extended Kalman filter (EKF) based interactive MM (IMM) algorithm whereas the other is an MM particle filter (PF).

Nevertheless, classical MM-based approaches rely on the strong assumption that the system can only switch between a finite number of *a priori* known models. Recently, Bayesian non-parametric (BNP) models have been introduced. They are mainly popular in statistics or machine learning [12]–[14]. These approaches make it possible to relax assumptions regarding the number of evolution models to be considered and the distributions of their parameters. Indeed, if the state transition matrix and/or the model noise and measurement covariance matrices are assumed to be unknown, their probability density functions (pdfs) can be modeled as Dirichlet process (DP) mixtures which can be seen as infinite mixtures of Gaussian distributions [12] [14]. This amounts to considering that the matrices to be estimated can switch between an unknown number of persistent modes. This approach has the advantage of being flexible but its drawback lies in the dimension of the model parameters to be learnt. It is all the higher as the state-vector size is large. In this paper, we suggest finding a compromise between the number of variables to be estimated and the flexibility of the algorithm. For this purpose, within each target class, we propose to categorize the motion models in families. For each of them, the state-transition and model-noise covariance matrices are characterized by a known functional form but they differ by a reduced set of unknown hyperparameters such as the model-noise variance or motion-model time constants. Only these hyperparameters thus need to be estimated by using non-parametric models called DPs.

Finally, the MM-based and the DP-based Bayesian algorithms are applied to maritime-target tracking. In this case, the classification consists in identifying if a target is non-maneuvering or potentially maneuvering. A comparative study between the three proposed approaches is then carried out in terms of computational cost and estimation performance.

Our paper is organized as follows: in section II, the problem statement is presented. Then, the multiclass MM-based and DP-based approaches are detailed in section III and section IV respectively. They are then applied to maritime-target tracking in section V where simulation results are presented. Finally, conclusions and perspectives are drawn in section VI.

In the following, $\otimes$ denotes the Kronecker product, ^{T} the transpose, $\delta_x(.)$ the Dirac distribution centered in x and I_N the identity matrix of size N. $blkdiag$ and $diag$ create a block diagonal matrix and a diagonal matrix respectively. In addition, $\sim$ stands for *is distributed according to* and $\mathcal{N}(x, \mu, \Sigma)$ is the Gaussian distribution for the variable x whose mean and covariance are μ and Σ respectively. The sequence $\{u_1, ..., u_l\}$ is denoted $u_{1:l}$.

II. Problem statement

A. System modeling only based on target dynamics

When tracking a maneuvering target, there is a high uncertainty about its evolution model. In this case, classifying the target in one of some predefined classes can help the practitioner to adjust the target dynamical model.

Let us assume that a target belongs to one among C target classes, denoted by $c \in \{1, ..., C\}$. This attribute does not vary over time and characterizes a type of target. We then assume that its trajectory in the xy-plane can be described by a finite number $r(c)$ of possible motion models denoted $\{M_1^c, ..., M_{r(c)}^c\}$. Within each class, the transition between the different motion models is described by a Markov chain whose transition probability matrix (TPM) is denoted by Π^c. If m_k^c denotes the motion model of the target at time k, the elements $\{\Pi_{ij}^c\}_{i=1,...,r(c)}^{j=1,...,r(c)}$ of Π^c satisfy:

$$\Pi_{ji}^c = Pr(m_{k+1}^c = M_i^c | m_k^c = M_j^c) \tag{1}$$

For the motion model m_k^c at time k, the system evolution model is described by:

$$\boldsymbol{x}_{k+1} = F^{m_k^c} \boldsymbol{x}_k + \boldsymbol{u}_k^{m_k^c} \tag{2}$$

where:

- the state vector $\boldsymbol{x}_k$ is defined for second-order and third-order motion models respectively as follows:

$$\boldsymbol{x}_k = [x_k, \dot{x}_k, y_k, \dot{y}_k]^T \; ; \; \boldsymbol{x}_k = [x_k, \dot{x}_k, \ddot{x}_k, y_k, \dot{y}_k, \ddot{y}_k]^T \tag{3}$$

  with x_k and y_k the positions, $\dot{x}_k$ and $\dot{y}_k$ the velocities and $\ddot{x}_k$ and $\ddot{y}_k$ the accelerations on the x and y dimension.
- $F^{m_k^c}$ denotes the transition matrix, $\boldsymbol{u}_k^{m_k^c}$ is a zero-mean white Gaussian noise with covariance matrix $Q^{m_k^c}$.

It should be noted that the functional forms of $F^{m_k^c}$ and $Q^{m_k^c}$ are different according to the type of motion model. For instance, among the possible system evolution models, the constant velocity (CV) [15] is defined by the following transition and covariance matrices:

$$F^{CV} = I_2 \otimes \begin{bmatrix} 1 & T \\ 0 & 1 \end{bmatrix} \; ; \; Q^{CV} = I_2 \otimes \sigma_{CV}^2 \begin{bmatrix} \frac{T^3}{2} & \frac{T^2}{2} \\ \frac{T^2}{2} & T \end{bmatrix} \tag{4}$$

with T the sampling period and σ_{CV}^2 the acceleration variance. When considering a Singer motion model [16], one has:

$$F^{Sin} = I_2 \otimes \begin{bmatrix} 1 & T & \frac{(\alpha T + \rho)}{\alpha^2} \\ 0 & 1 & \frac{(2-\rho)}{\alpha} \\ 0 & 0 & \rho + 1 \end{bmatrix} \; ; \; Q^{Sin} = I_2 \otimes \sigma_{Sin}^2 \tilde{Q}^{Sin} \tag{5}$$

where $\rho = e^{(-\alpha T)} - 1$ and $\alpha = \frac{1}{\tau_{Sin}}$ with τ_{Sin} the Singer time constant. σ_{Sin}^2 is the acceleration variance and $\tilde{Q}^{Sin}$ a matrix of size 3×3 and whose elements are functions of both α and T. For the sake of space, their expressions are not detailed but can be found in [16].

As an airborne radar usually provides the radar-to-target distance and the bearing angle, the measurement function is:

$$h(\boldsymbol{x}_k) = \begin{bmatrix} \sqrt{(x_k - x_r)^2 + (y_k - y_r)^2} \\ tan^{-1}(\frac{y_k - y_r}{x_k - x_r}) \end{bmatrix} \tag{6}$$

where $(x_r, \; y_r)$ are the radar coordinates which are known. The noisy measurement $\boldsymbol{y}_k$ and the state vector thus satisfy:

$$\boldsymbol{y}_k = h(\boldsymbol{x}_k) + \boldsymbol{v}_k \tag{7}$$

where the measurement noise $\boldsymbol{v}_k$, uncorrelated with $\boldsymbol{u}_k^{m_k^c}$, is a zero-mean white Gaussian noise with covariance matrix $R = diag(\sigma_d^2, \sigma_{ba}^2)$ where σ_d^2 and σ_{ba}^2 are the variances on the distance and bearing angle measurements respectively.

This system modeling only based on target dynamics is used in a wide range of approaches. Nevertheless, knowing target features such as the target dimension can be of real interest to improve the tracking performance. Therefore, we jointly estimate the target kinematic parameters and the target length.

B. System modeling including the target length

In practical cases, the dimensions of the target are not directly available. However, the range extent of a moving target, which is a function of both the target dimension and the relative geometry between the target and the sensor, can be estimated from an HRR radar. Under some assumptions, it can be related to the target length. In order to exploit the target extent measurements for any target orientation regarding the radar, the maritime-target shape is based on an elliptical model [10]. From this model, as illustrated by Fig. 1, it can be shown that the down-range extent of a target is defined as follows:

$$L^*(\phi, l) = l \sqrt{cos^2(\phi) + \left(\frac{b}{a}\right)^2 sin^2(\phi)} \tag{8}$$

where ϕ denotes the angle between the direction of the target and the radar-to-target LOS. In addition, l is the target length and $\frac{b}{a}$ is the ratio between the major and the minor axis lengths of the ellipse. As suggested by [10], the ratio $\frac{b}{a}$ is assumed to be known. In the framework of maritime target tracking, it can be considered that the target is oriented according to the same direction as the target velocity vector.

In addition, in practice, the down-range extent measurement is disturbed by an additive zero-mean Gaussian noise w_k with

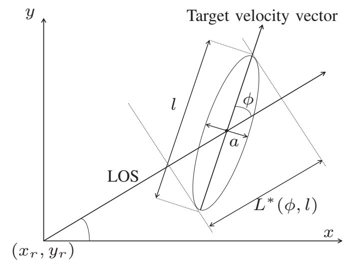

Fig. 1. Target elliptical model

variance σ_{dr}^2 and uncorrelated with $\boldsymbol{v}_k$ as well as $\boldsymbol{u}_k^{m_k^c}$. Thus, it can be shown that it is expressed as:

$$\begin{aligned} L_k &= L^*(\boldsymbol{x}_k, l) + w_k \\ &= \frac{l\sqrt{(\dot{y}_k\Delta_y + \dot{x}_k\Delta_x)^2 + \left(\frac{b}{a}\right)^2(\dot{y}_k\Delta_x - \dot{x}_k\Delta_y)^2}}{\sqrt{{\Delta_x}^2 + {\Delta_y}^2}\sqrt{\dot{x}_k^2 + \dot{y}_k^2}} + w_k \end{aligned} \quad (9)$$

where $\Delta_x = x_k - x_r$, $\Delta_y = y_k - y_r$.

In the remainder of the paper, given (2) and (9) an extended state vector which includes both the kinematic parameters and the target length is introduced. It satisfies:

$$\boldsymbol{X}_k = [\boldsymbol{x}_k^T \; l]^T \quad (10)$$

where l does not vary over time unlike $\boldsymbol{x}_k$.

In this case, for the motion model m_k^c at time k, the extended state vector evolves over time as follows:

$$\boldsymbol{X}_{k+1} = \boldsymbol{F}^{m_k^c}\boldsymbol{X}_k + \boldsymbol{U}_k^{m_k^c} \quad (11)$$

where $\boldsymbol{U}_k^{m_k^c} = [(\boldsymbol{u}_k^{m_k^c})^T \; 0]^T$ is the zero-mean extended model noise with covariance matrix $\boldsymbol{Q}^{m_k^c}$ and the state-transition and covariance matrices are defined by:

$$\boldsymbol{F}^{m_k^c} = blkdiag([F^{m_k^c} \; 1]) \; ; \; \boldsymbol{Q}^{m_k^c} = blkdiag([Q^{m_k^c} \; 0]) \quad (12)$$

As for the measurement equation, (7) becomes:

$$\boldsymbol{Y}_k = [\boldsymbol{y}_k^T \; L_k]^T = \boldsymbol{h}(\boldsymbol{X}_k) + \boldsymbol{V}_k \quad (13)$$

with $\boldsymbol{h}(\boldsymbol{X}_k) = [h(\boldsymbol{x}_k)^T \; L^*(\boldsymbol{x}_k, l)]^T$ and $\boldsymbol{V}_k = [\boldsymbol{v}_k^T \; w_k]^T$ the measurement noise with covariance matrix $\boldsymbol{R} = blkdiag(R, \sigma_{dr}^2)$.

Given the above state space representation (SSR) for the motion model m_k^c, target tracking can be done by sequentially estimating the state vector $\boldsymbol{X}_k$ by using the noisy observations $\boldsymbol{Y}_{1:k}$.

As depicted by (11), the system evolution model can switch from one motion model to another at each instant. To take it into account, multiple models algorithms can be used [17] [18]. For a given motion model, as the measurement equation (13) is non-linear, one of the following approaches can be used: an extended KF (EKF), a second-order EKF, a sigma-point KF such as the unscented KF [19], the central difference difference KF [20] and the cubature or the quadrature KF [21]. The EKF, which usually exhibits a good compromise between computational cost and estimation accuracy is usually preferred. Alternatively, if the non-linearity of the measurement function defined by (13) is high, a PF can be considered.

III. Joint Tracking and Classification Algorithm

Given (1), (11) and (13), the objective is to determine the actual target class c and to estimate the state vector $\boldsymbol{X}_k$ given the sets of kinematic measurements $\boldsymbol{y}_{1:k}$ and the target extent measurements $L_{1:k}$.

In a Bayesian context, the estimation of the state and the target class can be performed by using the maxima or the mean of the joint posterior distribution. This issue can be decomposed in two steps. First, the posterior distribution of the c^{th} target class can be sequentially computed as follows:

$$\begin{aligned} Pr(c|\boldsymbol{Y}_{1:k}) &= \frac{p(\boldsymbol{Y}_k|\boldsymbol{Y}_{1:k-1}, c)Pr(c|\boldsymbol{Y}_{1:k-1})}{p(\boldsymbol{Y}_k|\boldsymbol{Y}_{1:k-1})} \\ &= \frac{p(\boldsymbol{Y}_k|\boldsymbol{Y}_{1:k-1}, c)Pr(c|\boldsymbol{Y}_{1:k-1})}{\sum_{c=1}^{C} p(\boldsymbol{Y}_k|\boldsymbol{Y}_{1:k-1}, c)Pr(c|\boldsymbol{Y}_{1:k-1})} \end{aligned} \quad (14)$$

where at the initial time $\forall c \in \{1, ..., C\}$, $Pr(c) = \frac{1}{C}$.

Then, using the Bayes rule, the posterior pdf $p(\boldsymbol{X}_k|\boldsymbol{Y}_{1:k})$ is:

$$p(\boldsymbol{X}_k|\boldsymbol{Y}_{1:k}) = \sum_{c=1}^{C} p(\boldsymbol{X}_k|\boldsymbol{Y}_{1:k}, c)Pr(c|\boldsymbol{Y}_{1:k}) \quad (15)$$

At the initial time $p(l|c) = \mathcal{N}(l, l_0^c, P_0^c)$ and $p(\boldsymbol{x_0})$ is Gaussian. To address the problem described by (14) and (15), three methods are proposed. They all share the same architecture depicted by Fig. 2, but differ by the way the estimation within each class is performed. In the following of this section, two MM-based approaches are first presented: a multiclass IMM (MC-IMM) algorithm based on EKFs and a multiclass MM particle filter (MC-MMPF).

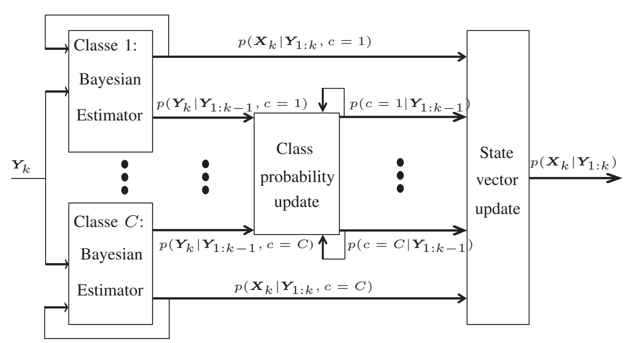

Fig. 2. Architecture of the proposed algorithms

A. Multiclass IMM filter

For this first approach, we propose to estimate $\boldsymbol{X}_k$ within each class by using an IMM algorithm. The latter consists in running a finite number of filters in parallel, each one based on a different state-model hypothesis. Here, EKFs are used. Their outputs are sequentially merged by using a cooperation strategy to prevent an exponential increase of the computational complexity. At each instant, the predictive and the posterior distributions are approximated one after the other by a mixture of Gaussian distributions. In our case, they are expressed as:

$$p(\boldsymbol{X}_k|\boldsymbol{Y}_{1:k-1}, c) \simeq \sum_{i=1}^{r(c)} \mu_{k|k-1}^{(i,c)} \mathcal{N}(\boldsymbol{X}_k, \boldsymbol{X}_{k|k-1}^{(i,c)}, P_{k|k-1}^{(i,c)}) \quad (16)$$

$$p(\boldsymbol{X}_k|\boldsymbol{Y}_{1:k}, c) \simeq \sum_{i=1}^{r(c)} \mu_k^{(i,c)} \mathcal{N}(\boldsymbol{X}_k, \boldsymbol{X}_{k|k}^{(i,c)}, P_{k|k}^{(i,c)}) \quad (17)$$

where $\boldsymbol{X}_{k|k-1}^{(i,c)}$ and $\boldsymbol{X}_{k|k}^{(i,c)}$ are the prediction and the estimation of the state vector $\boldsymbol{X}_k$ computed by the i^{th} EKF at time k. $\boldsymbol{P}_{k|k-1}^{(i,c)}$ and $\boldsymbol{P}_{k|k}^{(i,c)}$ are their corresponding error covariance matrices. In addition, the filter weights are updated recursively as follows:

$$\mu_{k|k-1}^{(i,c)} \propto \sum_{j=1}^{r(c)} \Pi_{ji}^{c} \mu_{k-1}^{(j,c)} \tag{18}$$

$$\mu_{k}^{(i,c)} \propto p(\boldsymbol{Y}_k|\boldsymbol{X}_k, c)\mu_{k|k-1}^{(i,c)} \tag{19}$$

The proportionality constant is adjusted so that:

$$\sum_{i=1}^{r(c)} \mu_{k|k-1}^{(i,c)} = \sum_{i=1}^{r(c)} \mu_{k}^{(i,c)} = 1.$$

Finally, (17) is substituted in (15) to yield the posterior distribution of the state vector.

As for the posterior distribution of the class $Pr(c|\boldsymbol{Y}_{1:k})$, it is recursively computed by using (14) with:

$$\begin{aligned} &p(\boldsymbol{Y}_k|\boldsymbol{Y}_{1:k-1}, c) \\ &= \int_{\boldsymbol{X}_k} p(\boldsymbol{Y}_k|\boldsymbol{X}_k, c) p(\boldsymbol{X}_k|\boldsymbol{Y}_{1:k-1}, c) d\boldsymbol{X}_k \\ &\underset{(16)}{\simeq} \sum_{i=1}^{r(c)} \mu_{k|k-1}^{(i,c)} \int_{\boldsymbol{X}_k} p(\boldsymbol{Y}_k|\boldsymbol{X}_k, c) \mathcal{N}(\boldsymbol{X}_k, \boldsymbol{X}_{k|k-1}^{(i,c)}, P_{k|k-1}^{(i,c)}) d\boldsymbol{X}_k \\ &\simeq \sum_{i=1}^{r(c)} \mu_{k|k-1}^{(i,c)} \mathcal{N}(\boldsymbol{Y}_k, \boldsymbol{Y}_{k|k-1}^{(i,c)}, S_k^{(i,c)}) \end{aligned} \tag{20}$$

with $\mathcal{N}(\boldsymbol{Y}_k, \boldsymbol{Y}_{k|k-1}^{(i,c)}, S_k^{(i,c)})$ the pdf of the i^{th}-EKF innovation for the IMM of the class c at time k and where $S_k^{(i,c)}$ and $\boldsymbol{Y}_{k|k-1}^{(i,c)}$ denote the innovation covariance matrix and the predicted measurement respectively. They are computed as follows:

$$\boldsymbol{Y}_{k|k-1}^{(i,c)} = \boldsymbol{h}(\boldsymbol{X}_{k|k-1}^{(i,c)}) \tag{21}$$

$$S_k^{(i,c)} = H^{(i,c)} P_{k|k-1}^{(i,c)} (H^{(i,c)})^T + \boldsymbol{R} \tag{22}$$

with $H^{(i,c)}$ the Jacobian matrix of the measurement function $\boldsymbol{h}$ evaluated at $\boldsymbol{X}_{k|k-1}^{(i,c)}$. Its elements are recalled in [10]. As a consequence, our first approach consists in combining (16)-(22).

B. Multiclass MMPF

As an alternative to the MC-IMM filter, we propose to jointly estimate within each class the continuous-valued states $\{\boldsymbol{x}_k, l\}$ and the motion model m_k^c by using particle filtering. More precisely, it can be observed that conditionally upon $\bar{\boldsymbol{x}}_k = [\boldsymbol{x}_k^T \; m_k^c]^T$, the state-space model is linear Gaussian with regard to the target size l. In this case, Rao-Blackwellized particle filters (RBPFs) are classically used. They are based on the following decomposition of the joint posterior pdf:

$$\begin{aligned} p(\bar{\boldsymbol{x}}_{0:k}, l|\boldsymbol{Y}_{1:k}, c) &= p(l|\bar{\boldsymbol{x}}_{0:k}, \boldsymbol{Y}_{1:k}, c) p(\bar{\boldsymbol{x}}_{0:k}|\boldsymbol{Y}_{1:k}, c) \\ &= p(l|\bar{\boldsymbol{x}}_{0:k}, L_{1:k}, c) p(\bar{\boldsymbol{x}}_{0:k}|\boldsymbol{Y}_{1:k}, c) \end{aligned} \tag{23}$$

where $p(l|\bar{\boldsymbol{x}}_{0:k}, L_{1:k}, c)$ is Gaussian. Thus, for each class, only $p(\bar{\boldsymbol{x}}_{0:k}|\boldsymbol{Y}_{1:k}, c)$ is estimated by particle filtering as follows:

$$\hat{p}(\bar{\boldsymbol{x}}_{0:k}|\boldsymbol{Y}_{1:k}, c) = \sum_{i=1}^{N_p} w_k^{(i,c)} \delta_{\bar{\boldsymbol{x}}_{0:k}^{(i,c)}}(\bar{\boldsymbol{x}}_{0:k}) \tag{24}$$

where the support points $\bar{\boldsymbol{x}}_{0:k}^{(i,c)}$ are sequentially generated according to a proposal distribution $q(\bar{\boldsymbol{x}}_k^{(i,c)}|\bar{\boldsymbol{x}}_{0:k-1}^{(i,c)}, \boldsymbol{Y}_{1:k}, c)$ and the so-called weights $\{w_k^{(i,c)}\}_{i=1,\dots,N_p}$ are computed to correct for the discrepancy between the actual posterior distribution and the proposal distribution. They can be recursively computed as:

$$\begin{aligned} \bar{w}_k^{(i,c)} &= w_{k-1}^{(i,c)} \frac{p(\boldsymbol{y}_k|\bar{\boldsymbol{x}}_k^{(i,c)}) p(L_k|\bar{\boldsymbol{x}}_{0:k}^{(i,c)}, L_{1:k-1}) p(\bar{\boldsymbol{x}}_k^{(i,c)}|\bar{\boldsymbol{x}}_{k-1}^{(i,c)}, c)}{q(\bar{\boldsymbol{x}}_k^{(i,c)}|\bar{\boldsymbol{x}}_{0:k-1}^{(i,c)}, \boldsymbol{Y}_{1:k}, c)} \\ w_k^{(i,c)} &= \frac{\bar{w}_k^{(i,c)}}{\sum_i \bar{w}_k^{(i,c)}} \end{aligned} \tag{25}$$

Then, it suffices to run a Kalman filter (KF) for each particle $\bar{\boldsymbol{x}}_{0:k}^{i}$ to compute in closed-form the conditional pdf:

$$p(l|\bar{\boldsymbol{x}}_{0:k}^{i}, L_{1:k}, c) = \mathcal{N}(l, \hat{l}_k^{(i,c)}, P_{k|k}^{(i,c)}) \tag{26}$$

where $\hat{l}_k^{(i,c)}$ and $P_{k|k}^{(i,c)}$ are the target length estimate and the corresponding error covariance matrix for the i^{th} KF, respectively. By inserting (24) and (26) into (23) and then integrating out $\bar{\boldsymbol{x}}_{0:k}$, it finally ensues:

$$\hat{p}(l|\boldsymbol{Y}_{1:k}, c) = \sum_{i=1}^{N_p} w_k^{(i,c)} \mathcal{N}(l, \hat{l}_k^{(i,c)}, P_{k|k}^{(i,c)}) \tag{27}$$

Given the distribution (27), the target length can be estimated. Concerning the class probability, it can be recursively expressed from (14) by first computing:

$$\begin{aligned} &p(\boldsymbol{Y}_k|\boldsymbol{Y}_{1:k-1}, c) \\ &= \int_l \int_{\bar{\boldsymbol{x}}_{0:k}} p(\boldsymbol{Y}_k|l, \bar{\boldsymbol{x}}_{0:k}, \boldsymbol{Y}_{1:k-1}, c) p(l, \bar{\boldsymbol{x}}_{0:k}|\boldsymbol{Y}_{1:k-1}, c) d\bar{\boldsymbol{x}}_{0:k} dl \end{aligned} \tag{28}$$

with $p(l, \bar{\boldsymbol{x}}_{0:k}|\boldsymbol{Y}_{1:k-1}, c) = p(l|\bar{\boldsymbol{x}}_{0:k}, \boldsymbol{Y}_{1:k-1}, c) p(\bar{\boldsymbol{x}}_{0:k}|\boldsymbol{Y}_{1:k-1}, c)$. Then, within the PF, the predictive distribution can be approximated by:

$$p(\bar{\boldsymbol{x}}_{0:k}|\boldsymbol{Y}_{1:k-1}, c) \simeq \sum_{i=1}^{N_p} w_{k|k-1}^{(i,c)} \delta_{\bar{\boldsymbol{x}}_{0:k}^{(i,c)}}(\bar{\boldsymbol{x}}_{0:k}) \tag{29}$$

with $w_{k|k-1}^{(i,c)} \propto w_{k-1}^{(i,c)} \frac{p(\bar{\boldsymbol{x}}_k^{(i,c)}|\bar{\boldsymbol{x}}_{k-1}^{(i,c)}, c)}{q(\bar{\boldsymbol{x}}_k^{(i,c)}|\bar{\boldsymbol{x}}_{0:k-1}^{(i,c)}, c, \boldsymbol{Y}_{1:k})}$.

Replacing (29) into (28) and taking into account conditional independencies lead to:

$$\begin{aligned} &p(\boldsymbol{Y}_k|\boldsymbol{Y}_{1:k-1}, c) \\ &\approx \int_l \sum_{i=1}^{N_p} w_{k|k-1}^{(i,c)} p(L_k|l, \bar{\boldsymbol{x}}_{0:k}^{(i,c)}) p(y_k|\bar{\boldsymbol{x}}_k^{(i,c)}) p(l|\bar{\boldsymbol{x}}_{0:k}^{(i,c)}, L_{1:k-1}) dl \\ &\approx \sum_{i=1}^{N_p} w_{k|k-1}^{(i,c)} p(y_k|\bar{\boldsymbol{x}}_k^{(i,c)}) \int_l p(L_k|l, \bar{\boldsymbol{x}}_{0:k}^{(i,c)}) p(l|\bar{\boldsymbol{x}}_{0:k}^{(i,c)}, L_{1:k-1}) dl \\ &\approx \sum_{i=1}^{N_p} w_{k|k-1}^{(i,c)} p(y_k|\bar{\boldsymbol{x}}_k^{(i,c)}) \mathcal{N}(l, \hat{l}_{k|k-1}^{(i,c)}, s_k^{(i,c)}) \end{aligned} \tag{30}$$

where $\hat{l}_{k|k-1}^{(i,c)}$ is the predicted length associated to the i^{th} particle at time k and $s_k^{(i,c)}$ is its variance.

Note that in practice, we have used as proposal distribution $q(\bar{\boldsymbol{x}}_k^{(i,c)}|\bar{\boldsymbol{x}}_{0:k-1}^{(i,c)}, \boldsymbol{Y}_{1:k}, c) = p(\bar{\boldsymbol{x}}_k^{(i,c)}|\bar{\boldsymbol{x}}_{k-1}^{(i,c)}, c)$.

IV. EXTENSION TO UNKNOWN MODEL PARAMETERS

The above algorithms rely on the strong assumption that the target of a given class can only switch between a finite number of motion models whose model-noise variances should be *a priori* set. However, these variances cannot be finely tuned in practice whereas they may severely impact the tracking performance. A standard solution to this problem is to increase the number of models in the MM structure by representing a given maneuver by several models characterized by different model-noise variance values. Its main limitation is that using too many competing models in parallel can degrade the estimation performance, as suggested in [17]. In order to relax this constraint on the model set design, non-parametric models have been recently considered [12], [14]. The idea is to impose no prior on the cardinality of the models as well as their parameters so that the latter are learnt directly from the data. In [12] and [14], the distributions of either the model control input or the model noise are assumed unknown and modeled as infinite mixture of distributions. Conversely, the state transition matrix is assumed to be known.

The specificity of our approach is the following: we consider that the target motion models can be categorized in a finite number of model families (CV, constant acceleration, constant turn, Singer, etc.) corresponding to a given maneuver mode. All the models within a class share the same known functional form but differ from a model-noise variance parameter denoted γ_k. Only the latter is allowed to switch between an infinite number of values. The proposed hierarchical model thus includes a discrete variable that indicates the model family. Conditionally to it, the distribution of the time-switching model-noise variance is modeled by a DP. The system evolution is hence described by a mixture of DPs. On the basis of our hierarchical model, Bayesian inference of the target class, the current model family, the state vector and the model-noise variance is performed at each instant by using particle filtering.

A. DP principle

Let us consider a set of variables $\{\gamma_k\}_{k\geq 0}$ assumed to be independent and identically distributed according to a distribution G. Bayesian non-parametric modeling consists in considering that G is unknown and is assigned a prior distribution. In this paper, we consider a class of prior termed DPs that have the advantage of being very flexible and making the inference easily tractable thanks to the so-called polya-urn representation. DPs are defined as distributions over the space of probability measures [12]. They are uniquely characterized by a base distribution G_0 and a scale factor α_0. If G is the unknown distribution of the variables $\{\gamma_k\}_{k\geq 0}$, one has:

$$G \sim DP(G_0, \alpha_0) \tag{31}$$

The realizations G of a DP are infinite distributions. By using the stick-breaking representation, they can be expressed as:

$$G(\gamma_k) = \sum_{j=1}^{+\infty} \pi_j \delta_{\boldsymbol{U}_j}(\gamma_k) \tag{32}$$

where $\boldsymbol{U}_j \sim G_0$, $\pi_j = \beta_j \prod_{l=1}^{j-1}(1-\beta_l)$ and $\beta_j \sim \mathcal{B}(1, \alpha_0)$, where $\mathcal{B}$ stands for the Beta law. Note that (32) defines a probability measure since $\sum_{j=1}^{+\infty} \pi_j = 1$.

Estimating G is an infinite-dimensional problem. However, Blackwell *et al.* showed in [22] that the DP inference procedure boils down to the estimation of the latent variable γ_k. Indeed, the predicted distribution of γ_k given the latent variables $\gamma_{1:k-1}$ can be directly computed by marginalizing G. It leads to the Polya urn representation:

$$p(\gamma_k|\gamma_{1:k-1}, \alpha_0) = \frac{1}{\alpha_0 + k - 1} \sum_{j=1}^{k-1} \delta_{\gamma_j}(\gamma_k) + \frac{\alpha_0}{\alpha_0 + k - 1} G_0(\gamma_k) \tag{33}$$

It can be interpreted as a reinforcement property: given the previous latent variables $\gamma_{1:k-1}$, a new sample can either be drawn from the distribution G_0 with probability $\frac{\alpha_0}{\alpha_0+k-1}$ or take the same value as a previous sample with probability $\frac{k-1}{\alpha_0+k-1}$. Therefore, the scale parameter plays a key role. If α_0 is small, the same value of γ_k is drawn several times whereas if α_0 tends to infinity, the samples become *iid* from G_0.

In the next subsection, the proposed hierarchical model based on mixtures of DPs is detailed.

B. Proposed hierarchical model

Let $z_k^c \in \{1, ..., f(c)\}$ denote the index of the actual motion-model family at time k for the class c and $f(c)$ the number of model families in this class. Here, the sequence $\{z_k^c\}_{k>0}$ is assumed to be a Markov chain with TPM denoted as $\pi^c = \{\pi_{ij}^c\}_{i=1,...,f(c)}^{j=1,...,f(c)}$. Note that unlike the previous MM-based approaches, the index z_k^c does not refer to a well-defined model but to a family composed of an infinity of models corresponding to different values for the variance parameter γ_k.

Conditionally to z_k^c, the distribution of γ_k is assigned a DP prior. The specificity of our work is hence that we consider as many DPs as possible model families for a given target class. Their realizations are denoted as $\{G^{c,m}\}_{m=1,...,f(c)}^{c=1,...,C}$. Each DP is characterized by its own base distribution $G_0^{c,m}$ and its scale parameter $\alpha_0^{c,m}$.

Given the above considerations, the relationships between z_k^c, $G^{c,m}$, γ_k, $\boldsymbol{X}_k$ and $\boldsymbol{Y}_k$ can be described by the following hierarchical model:

$$z_k^c | z_{k-1}^c \sim \pi^c_{z_k^c z_{k-1}^c} \tag{34}$$

$$G^{c,m} \sim \mathcal{DP}(G_0^{c,m}, \alpha_0^{c,m}) \text{ for } \ m = 1, ..., f(c) \tag{35}$$

$$\gamma_k | \{z_k^c, \{G^{c,m}\}_{m=1,...,f(c)}\} \sim G^{c,z_k^c}(\gamma_k) \tag{36}$$

$$\boldsymbol{X}_k | \{\boldsymbol{X}_{k-1}, \gamma_k, z_k^c\} \sim p(\boldsymbol{X}_k | \boldsymbol{X}_{k-1}, \gamma_k, z_k^c) \tag{37}$$

$$\boldsymbol{Y}_k | \boldsymbol{X}_k \sim p(\boldsymbol{Y}_k | \boldsymbol{X}_k) \tag{38}$$

Based on the Polya urn representation, the unknown distributions $\{G^{c,m}\}_{m=1,...,f(c)}$ can be integrated out of this hierarchical model. However, the switching between the different model families has to be taken into account. The predictive distribution of γ_k becomes:

$$\gamma_k | \{\gamma_{1:k-1}, z_k^c, c\} \sim \frac{1}{\alpha_0^{z_k^c} + n_{z_k^c}} \sum_{\substack{j=1 \\ s.t.\ z_j^c = z_k^c}}^{k-1} \delta_{\gamma_j}(\gamma_k) + \frac{\alpha_0^{z_k^c}}{\alpha_0^{z_k^c} + n_{z_k^c}} G_0^{z_k^c}(\gamma_k) \tag{39}$$

where $n_{z_k^c} = \sum_{j=1}^{k-1} \delta_{z_k^c}(z_j^c)$ is the number of times the model family z_k^c has previously appeared.
The hierachical model defined by (34)-(38) thus reduces to (34), (39), (37), and (38) as depicted in Fig. 3.

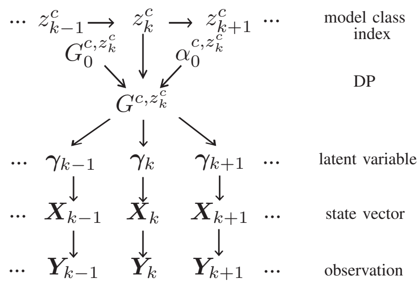

Fig. 3. Graphical representation of the hierarchical model

The objective is then, for each class, to on-line estimate the joint posterior distribution of all the unknown parameters $p(l, \boldsymbol{x}_{0:k}, z_{0:k}^c, \gamma_{0:k}|\boldsymbol{Y}_{1:k}, c)$. The latter does not admit a closed-form expression due to the non-linearity and non-Gaussianity of the proposed model. Therefore we use particle filtering techniques. Similarly to section III, the hierarchical model is linear Gaussian for the target length l conditionally upon $\boldsymbol{x}_{0:k}$, $z_{0:k}^c$ and $\gamma_{0:k}$. As a consequence, for each class, we propose to run a particle filter to address the estimation of the nonlinear states $\boldsymbol{x}_{0:k}$, $z_{0:k}^c$, $\gamma_{0:k}$ while the target length is optimally dealt with Kalman filtering. As for the propagation of the particles, the easiest way to proceed is to simulate them sequentially according to the prior model (34), (37), (39). Then, the particle weights are merely proportional to the likelihood $p(\boldsymbol{y}_k|\boldsymbol{x}_k^{(i,c)})p(L_k|\boldsymbol{x}_{0:k}^{(i,c)}, \gamma_{0:k}^{(i,c)}, z_{0:k}^{(i,c)}, L_{1:k-1})$. However, a great number of particles is necessary to yield a good approximation of the highly multi-dimensional posterior pdf. As an alternative, we have considered an approximation of the optimal proposal distribution [23]:

$$\begin{aligned} &q(\gamma_k^{(i,c)}, \boldsymbol{x}_k^{(i,c)}, z_k^{(i,c)}|\gamma_{0:k-1}^{(i,c)}, \boldsymbol{x}_{0:k-1}^{(i,c)}, z_{0:k-1}^{(i,c)}, \boldsymbol{y}_{1:k}^{(i,c)}, c) \\ &= q(\gamma_k^{(i,c)}|\gamma_{0:k-1}^{(i,c)}, \boldsymbol{x}_{0:k}^{(i,c)}, z_k^{(i,c)}, \boldsymbol{y}_{1:k}, c) \\ &\quad \times q(\boldsymbol{x}_k^{(i,c)}|\boldsymbol{x}_{0:k-1}^{(i,c)}, z_k^{(i,c)}, \boldsymbol{y}_{1:k}, c) Pr(z_k^{(i,c)}|z_{k-1}^{(i,c)}) \end{aligned} \tag{40}$$

Finally, as for the estimation of the class, the same expression as in (25) is used but the expression of the predictive weights is modified as follows:

$$\begin{aligned} &w_{k|k-1}^{(i,c)} \propto \\ &w_{k-1}^{(i,c)} \frac{p(\boldsymbol{x}_k^{(i,c)}|\boldsymbol{x}_{k-1}^{(i,c)}, \gamma_k^{(i,c)}, c) p(\gamma_k^{(i,c)}|\gamma_{0:k-1}^{(i,c)}, c)}{q(\gamma_k^{(i,c)}, \boldsymbol{x}_k^{(i,c)}|\gamma_{0:k-1}^{(i,c)}, \boldsymbol{x}_{0:k-1}^{(i,c)}, z_{0:k}^{(i,c)}, \boldsymbol{y}_{1:k}^{(i,c)})} \end{aligned} \tag{41}$$

V. Application to maritime-target tracking

A. Preliminary step: target class and model settings

Before analyzing the relevance of our approaches, let us define the type of target classes that are considered. According to Table I where the target lengths and the maximal accelerations are given for various target types, it can be deduced that a target is assumed to be potentially[1] maneuvering if its length is small enough.

Target type	Target length (m)	maximal acceleration	Target class
Freighter	≥ 100	$0.02g$	Non-maneuvering targets
Tanker	≥ 50	$0.02g$	
Ocean-going tug	≥ 50	$0.02g$	
Fiching vessels	≈ 20	$0.1g$	Maneuvering Targets
Rubber boats	≈ 10	$0.4g$	
Jetski	≈ 3	$0.5g$	
Pleasure boats	≈ 10	$0.2g$	

TABLE I
MARITIME TARGET FEATURES

In the following, a maritime target thus belongs to one of the $C = 2$ following classes:

- non-maneuvering targets,
- potentially maneuvering targets.

Let us now select the number and the type of motion models in each class. For the non-maneuvering target class, $r(1) = 1$: the motion model M_1^1 is hence a CV with model-noise standard deviation (std) denoted by $\sigma_{CV,1}$. Concerning the maneuvering-target tracking, we suggest combining $r(2) = 2$ models: M_1^2 is a CV motion whose std is $\sigma_{CV,2}$ and M_2^2 is a Singer motion model whose model-noise std and time constant are $\sigma_{Sin,2}$ and $\tau_{Sin,2}$. The switching between both is then described by (1).

B. Simulation protocol

To analyze the relevance of the three proposed approaches, a freighter of 120 m and a rubber boat of 10 m, denoted target 1 and target 2 respectively, are separately tracked.
At each instant, the trajectory of the target 1 is generated from a CV motion model whose acceleration std $\sigma_{CV,1}$ can switch between 5×10^{-2} $m.s^{-3/2}$ and 0.2 $m.s^{-3/2}$. The probability to change from one value to another is 0.02.
Concerning target 2, its trajectory is generated from a two-state Markov chain whose transition probability matrix is $\begin{bmatrix} 0.98 & 0.02 \\ 0.1 & 0.9 \end{bmatrix}$. The first state characterizes a CV motion model whereas the second state is a Singer motion model. As long as the target is described by the same model family, the corresponding model-noise std remains unchanged and can take one among the following values with an equiprobable way. For the CV model, $\sigma_{CV} \in \{10^{-1}; 2 \times 10^{-1}\}$ $m.s^{-3/2}$ and for the Singer model $\sigma_{Sin} \in \{1; 2; 3; 4; 5\} m.s^{-2}$ and $\tau_{Sin} = 15$ s.
Target trajectories are estimated from noisy radar measurements which consist of both position and target extent measurements. Note that for the measurement noise stds of the range and bearing angle, three different configurations are tested:

- *Conf. 1*: $\sigma_d = 10$ m, $\sigma_{ba} = 0.001$ rad.
- *Conf. 2*: $\sigma_d = 10$ m, $\sigma_{ba} = 0.005$ rad.
- *Conf. 3*: $\sigma_d = 20$ m, $\sigma_{ba} = 0.001$ rad.

In addition, the model-noise std of the down-range extent is $\sigma_{dr} = 5$ m and $T = 1$ s. Note that at the initial time, $l_0^1 = 120$ m, $P_0^1 = 400$ m^2 and $l_0^2 = 10$ m, $P_0^2 = 400$ m^2.
One trajectory realization for target 2 and the associated radar measurements are represented in Fig. 4.

[1]The term 'potentially' is used because, most of the time, maneuvering targets do not actually maneuver.

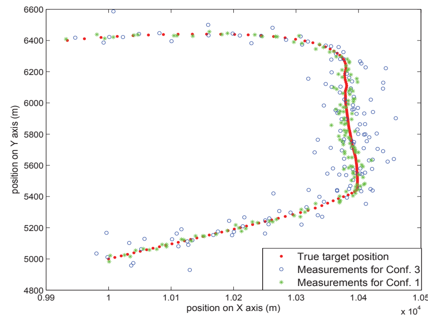

Fig. 4. Trajectory of target 2 and corresponding radar measurements

The three proposed approaches are designed as follows:

Multiclass IMM algorithm (*MC-IMM*):

The model parameters are: $\sigma_{CV,1} = \sigma_{CV,2} = 0.2\ m.s^{-3/2}$, $\sigma_{Sin,2} = 5\ m.s^{-2}$ and $\tau_{Sin,2} = 15\ s$. In addition, the TPM is set at[2]: $\Pi^{c=2} = \begin{bmatrix} 0.98 & 0.02 \\ 0.1 & 0.9 \end{bmatrix}$.

Multiclass MMPF-based algorithm (*MC-MMPF*):

For both classes, the model-parameter setting is the same as in MC-IMM. Moreover, the algorithm is run with $N_p = 3000$.

Algorithm based on the mixture of DPs (*MDP*):

For each class, the model-noise variance γ_k corresponding to the model family z_k^c is estimated. For the first class, $f(1) = 1$. $z_k^c = 1$ thus refers to a CV motion model, whereas for the second class $f(2) = 2$ so that $z_k^c \in \{1, 2\}$ refers to either a CV motion model or a Singer motion model. In this latter case, the model-family Markov chain is characterized by the following TPM: $\pi^{c=2} = \begin{bmatrix} 0.98 & 0.02 \\ 0.1 & 0.9 \end{bmatrix}$. As suggested in [12], the DP base distribution G_0 is defined as an inverse $Gamma$ conjugate prior $\Gamma(a_{z_k^c}, b_{z_k^c})$ on the *MDP* precision parameter. In order to consider a weakly informative setting, for the first target class: $a_1 = 4$, $b_1 = 40$. For the second target class, $a_1 = 4$, $b_1 = 40$ and $a_2 = 10$, $b_2 = 0.01$. Finally, the algorithm is run with $N_p = 3000$.

The results presented in the sequel are obtained from trajectories of 200 samples averaged over 100 Monte Carlo simulations.

C. Simulation results

In the following, we give some comments about the computational costs, the relevance of the algorithms concerning the class estimation as well as the position estimation and the target length estimation.

Computational cost:

Regarding the tests that have been performed, compared to a single-model based EKF filter or an EKF-based IMM that do not include classification, the computational cost of *MC-IMM* is only slightly higher. Nevertheless, concerning *MC-MMPF*, its complexity is more significant (around 50 times higher than *MC-IMM* when $N_p = 3000$) and is closely related to the number of particles that is used. Finally, the computational cost of *MDP* is the highest among all the proposed approaches (around 5 times higher than *MC-MMPF*). Note that the computational cost is not related to the classification since the calculations can be done using parallel computing for each class.

[2] It corresponds to a mean sojourn time of $50T$ and $10T$ in the first and the second model respectively.

Class estimation:

According to Fig. 5, where the class probabilities for the three proposed approaches are represented for the 40 first samples, using both kinematic and target extent measurement allows the target class to be well-identified. The convergence is rather fast and similar for the three proposed approaches. More precisely, because of the estimation of the model-noise variance, the convergence of *MDP* is the fastest. It should be noted that the clear-cut decision directly stems from the simulation protocol. Indeed, we have on purpose considered target lengths that clearly categorize them in one of the classes so as to better emphasize the influence of this information on the JTC. Moreover, due the model switching probabilities, it at worst takes a few iterations for target 2 to be maneuvering. In practice, for a target of medium length that does not maneuver during a long time period, the classification can take far more iterations.

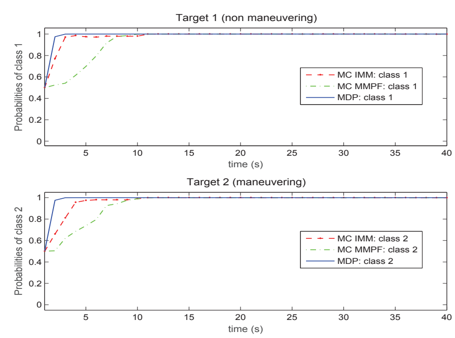

Fig. 5. Target class probabilities averaged over 100 Monte Carlo simulations

Position estimation:

The root mean square errors (RMSEs) on the positions for the three proposed approaches are compared with:

1/ the RMSE related to the measurement noise, i.e. without applying any filtering algorithm. It is denoted *Meas.*.

2/ the RMSE when using an EKF, denoted *Ref.*, based on the true motion model and set with the true model-noise std.

3/ the RMSE when using an *IMM* without classification combining two EKFs [17]. The first one is based on a CV motion model with $\sigma_{CV} = 2.10^{-1}\ m.s^{-\frac{3}{2}}$. The second one is based on a Singer motion model with $\sigma_{Sin} = 5\ m.s^{-2}$ and $\tau_{Sin} = 15\ s$.

Config.	*Meas.*	*Ref.*	*IMM*	*MC-IMM*	*MC-MMPF*	*MDP*
Conf. 1	15.33	7.88	8.62	8.16	8.27	**8.04**
Conf. 2	53.91	26.44	27.59	27.01	26.95	**26.62**
Conf. 3	59.25	33.43	34.91	34.37	34.23	**33.67**

TABLE II

RMSEs FOR TARGET 1 (NON-MANEUVERING TARGET)

Config.	*Meas.*	*Ref.*	*IMM*	*MC-IMM*	*MC-MMPF*	*MDP*
Conf. 1	14.75	8.08	8.92	8.91	8.78	**8.43**
Conf. 2	54.23	27.57	28.46	28.43	28.35	**27.85**
Conf. 3	60.68	34.32	35.68	35.66	35.32	**34.77**

TABLE III

RMSEs FOR TARGET 2 (POTENTIALLY MANEUVERING TARGET)

According to Table II and III, compared to *IMM*, the three proposed approaches have better performance for position estimation. In particular, as the model-noise variance is estimated with *MDP* at each instant, this approach outperforms the others for which the variance is set to a predefined value. In addition, *MC-MMPF* is slightly better than *MC-IMM* due to the non-linearity of the measurement function. Finally, one can remark than *MC-IMM* and *IMM* have close performance when dealing with the maneuvering target but differ for the non-maneuvering one. Indeed, for target 1, if the classification is correct, both *IMM* and *MC-IMM* are equivalent, whereas for target 2, *MC-IMM* reduces to a single CV-based EKF. This latter is then better than *MC-IMM* because, due to the IMM mixing strategy, the weights in favor of a given model are not necessarily clear-cut.

Infuence of the size estimation:

Finally, the target size estimation for one realization of the trajectory of target 1 (non-maneuvering) and target 2 (maneuvering) respectively obtained with Conf. 2 is analyzed.

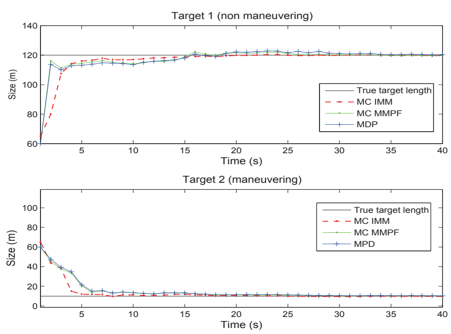

Fig. 6. Target size estimation: averaged over 100 Monte Carlo simulations

As depicted in Fig. 6, the target length estimation converges quickly to the true value. This characteristic is partly the cause of the fast convergence of the target-class probabilities. Indeed, as depicted by Fig. 7 for *MC-IMM* approach, without considering the target length estimation, the class probability convergence is slower. Therefore, the resulting RMSE is slightly higher than the one obtained with target extent measurements.

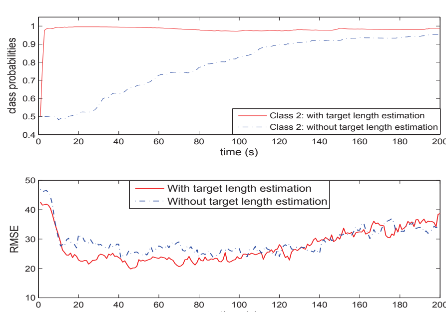

Fig. 7. Comparison of the *MC-IMM* performances with and without target extent measurements

VI. Conclusions and Perspectives

New JTC algorithms that take into account the target extent measurement are proposed. First, a multiclass EKF-based IMM filter and a multiclass MMPF are derived. Then, to alleviate the uncertainty on the time-varying model-noise variance, a new DP-based non-parametric model is introduced. The three proposed approaches are applied to maritime-target tracking. They are compared one another and with an IMM algorithm. It is shown that the DP-based algorithm outperforms the other algorithms. Nevertheless, this is at the cost of a high computational cost. As a perspective, we plan to test our approaches with real radar data and to generalize it to multitarget tracking.

References

[1] W. Mei, G.-L. Shan, and X. R. Li, “Simultaneous Tracking and Classification: A Modularized Scheme,” *IEEE Trans. on Aerospace and Electronics Systems*, vol. 43, pp. 581–599, 2007.

[2] W. Cao, J. Lan, and X. R. Li, “Extended Object Tracking and Classification based on Recursive Joint Decision and Estimation,” in *Int. Conf. on Information Fusion*, 2013, pp. 1670–1677.

[3] J. Lan and X. R. Li, “Joint Tracking and Classification of Extended Object Using Random Matrix,” in *Int. Conf. on Information Fusion*, 2013, pp. 1550–1557.

[4] W. Cao, J. Lan, and X. R. Li, “Joint Tracking and Classification of Extended Object Based on Support Functions,” in *Int. Conf. on Information Fusion*, 2014, pp. 1–8.

[5] W. Cao, J. Lan, and X. R. Li, “Joint Tracking and Classification of Extended Object Based on Recursive Joint Decision and Estimation Using Multi-Sensor Data,” in *Int. Conf. on Information Fusion*, 2014, pp. 1–8.

[6] B. Ristic, N. Gordon, and A. Bessell, “On Target Classification Using Kinematic Data,” *Information Fusion*, pp. 15–21, 2003.

[7] S. Challa and G. W. Pulford, “Joint Target Tracking and Classification Using Radar and ESM Sensors,” *IEEE Trans. on Aerospace and Electronics Systems*, vol. 37, pp. 1039–1055, 2001.

[8] D. Angelova and L. Mihaylova, “Sequential Monte Carlo Algorithms for Joint Target Tracking and Classification Using Kinematic Radar Information,” in *Int. Conf. on Information Fusion*, 2004, pp. 709–716.

[9] X. R. Li, M. Yang, and J. Ru, “Joint Tracking and Classification based on Bayes Joint Decision and Estimation,” in *Int. Conf. on Information Fusion*, 2007.

[10] D. J. Salmond and M. C. Parr, “Track Maintenance Using Measurements of Target Extent,” *IEE Proceedings of Radar, Sonar and Navigation*, vol. 150, pp. 389–395, 2003.

[11] B. Ristic and D. J. Salmond, “A Study of Nonlinear Filtering Problem for Tracking an Extended Target,” in *Int. Conf. on Information Fusion*, 2004.

[12] F. Caron, M. Davy, A. Doucet, E. Duflos, and P. Vanheeghe, “Bayesian Inference for Linear Dynamic Models with Dirichlet Process Mixtures,” *IEEE Trans. on Signal Processing*, vol. 56, pp. 71–84, 2008.

[13] E. Fox, E. B. Sudderth, M. I. Jordan, and A. Willsky, “Bayesian Nonparametric Methods for Learning Markov Switching Processes,” *IEEE Signal Processing Magazine*, vol. 27, pp. 43–54, 2010.

[14] E. Fox, E. B. Sudderth, M. I. Jordan, and A. Willsky, “Bayesian Nonparametric Inference of Switching Dynamic Linear Models,” *IEEE Trans. on Signal Processing*, vol. 59, pp. 1569–1585, 2011.

[15] X. R. Li and V. P. Jilkov, “Survey of Maneuvering Target Tracking. Part 1. Dynamic Models,” *IEEE Trans. on Aerospace and Elec. Syst.*, vol. 39, pp. 1333–1364, 2003.

[16] R. A. Singer, “Estimating Optimal Tracking Filter Performance for Manned Maneuvering Targets,” *IEEE Trans. on Aerospace and Elec. Syst.*, vol. 6, pp. 473–483, July 1970.

[17] Y. Bar-Shalom and X. R. Li, *Multitarget-Multisensor Tracking: Principles and Techniques*, YBS Publishing, Storrs, 1995.

[18] X. R. Li and V. P. Jilkov, “Survey of Maneuvering Target Tracking. Part V: Multiple Model Methods,” *IEEE Trans. on Aerospace and Elec. Syst.*, vol. 41, pp. 1255–1321, Oct. 2005.

[19] E. A. Wan and R. Van de Merwe, *Chapter 7: The Unscented Kalman Filter, in Kalman Filtering and Neural Networks*, Wiley, 2001.

[20] K. Ito and K. Xiong, “Gaussian Filters for Non-Linear Filtering Problems,” *IEEE Trans. on Automatic Control*, vol. 45, pp. 910–927, 2000.

[21] I. Arasaratnam and S. Haykin, “Cubature Kalman Filters,” *IEEE Trans. on Automatic Control*, vol. 54, pp. 1254–1259, 2009.

[22] D. Blackwell and B. MacQueen, “Ferguson Distributions via Polya Urn Schemes,” *The annals of statistics*, vol. 1, pp. 353–355, 1973.

[23] A. Doucet, N. de Freitas, and N. Gordon, *Sequential Monte Carlo Methods in Practice*, Springer Verlag, 2001.